Catalytic Assessment of the Glycine-Rich Loop of the v-Fps Oncoprotein Using Site-Directed Mutagenesis†

T. John Hirai, Igor Tsigelny, and Joseph A. Adams*

Department of Pharmacology, University of California, San Diego, La Jolla, California 92093-0506

Received May 30, 2000; Revised Manuscript Received August 21, 2000

ABSTRACT: The three glycine residues in the glycine-rich loop of the oncoprotein, v-Fps, were mutated to determine the function of these highly conserved residues in catalysis. The kinase domains of six mutants (G928A,S, G930A,S, and G933A,S) and the wild-type enzyme were expressed and purified as fusion proteins of glutathione-*S*-transferase in *Escherichia coli*, and their catalytic properties were assessed using steady-state kinetic, inhibition, viscosity and autophosphorylation studies. Although both G928A and G930A had no detectable activity toward the substrate peptide (EAEIYEAIE), the other mutants had apparent, but varying activities. G930S lowered the rate of phosphoryl transfer by 130-fold while G928S and G933S had smaller (6−9-fold) reductions in this step. These effects on catalytic function parallel the reductions in turnover and autophosphorylation but, for G933S and G933A, net product release is still rate limiting at saturating substrate and ATP concentrations. On the basis of K_I measurements, the effects on turnover for these mutants may be due to improved ADP affinity. While ADP affinity is reduced 2- and 3-fold for G928S and G930S, the affinity of this product is increased by 22- and 7-fold for G933S and G933A. In contrast, ATP affinity is enhanced by 5-fold for G928S and G933S and is reduced by less than 2-fold for G930S. These complex, differential effects on nucleotide binding indicate that the glycines influence the relative affinities of ADP and ATP. On the basis of the results of serine replacements, Gly-928 and Gly-930 *enhance* ADP affinity by 9- and 2-fold compared to ATP affinity whereas Gly-933 *diminishes* ADP affinity by approximately 4-fold compared to ATP affinity. These findings demonstrate that the functions of the loop lie not only in modulating the rate of the phosphoryl transfer step but also in balancing the relative affinities of ATP and ADP. These effects on nucleotide specificity may be a contributing element for the stabilization of the phosphoryl transition state and may also facilitate quick release of bound products.

The nucleotide-binding pockets of protein kinases contain a loop segment rich in glycine residues. This region, known as the glycine-rich loop (GRL),[1] includes the general consensus sequence, Gly-X-Gly-X-X-Gly, where X is variable. While the second glycine is strictly conserved, 95 and 85% of all protein kinases have glycines in the first and third positions of this sequence, respectively (*1*). Based on X-ray crystallographic results, the glycines of the GRL appear to play a role in binding ATP, but this function must be indirect in some cases. For example, in protein kinase A (PKA), only the first and third glycines of the GRL (L_{49}GTGSFGRV) make direct interactions with the nucleotide. The backbone amides of Gly-50 and Gly-55 interact with the ribose and β phosphate, but Gly-53 makes no direct contact with ATP (*2*, *3*). In comparison, none of the glycines in the GRL of the active kinase domain of the Insulin receptor (InRK) make direct contact with ATP (*4*). While direct involvement of the glycines in nucleotide binding is uncertain, other residues in the GRL make important contacts. For example, the backbone amide of Ser-53 in PKA interacts with the γ phosphate while Leu-49 and Val-57 interact with the adenine ring. In the InRK, the amide backbone of Ser-1006 in the GRL (L_{1002}GQGSFGMV) contacts the β phosphate of ATP. While the GRL may be ideally suited to position these residues for nucleotide stabilization, the loop could serve other global functions. The GRLs of protein kinases link together two β strands in the small nucleotide-binding domain. The turn offered by the glycines may be important for stabilizing this region of the protein. Furthermore, it is possible that the GRL acts as a "lid" that closes the nucleotide pocket (*1*, *2*), perhaps limiting access of water and decreasing the competitive hydrolysis reaction (ATPase). In one example, serine substitution at Gly-50 and Gly-52 in PKA increases the intrinsic ATPase rate by more than 1 order of magnitude (*5*), although both mutations cause 20- and 300-fold decreases in the rates of substrate phosphorylation (*6*).

The GRLs of protein kinases display varying levels of flexibility in the crystal form depending on the nature of the ligands bound and the phosphorylation state of a distal loop segment known as the "activation" loop. The binding of ATP to PKA, complexed with a peptide inhibitor, lowers the B factors for the GRL residues, suggesting that loop movement is more limited when nucleotide and metal are present (*2*, *7*, *8*). The binding of ATP alters significantly the susceptibility

† This work was supported by an NIH grant (CA 75112).

* To whom correspondence should be addressed. Phone: (858) 822-3360. Fax: (858) 822-3361. E-mail: joeadams@ucsd.edu.

[1] Abbreviations: GRL, glycine-rich loop; GST, glutathione-*S*-transferase; GST-kin, fusion protein of GST and the kinase domain of v-Fps; InRK, active kinase domain of the insulin receptor; Mops, 3-[*N*-morpholino] propanesulfonic acid; PhK, kinase domain of phosphorylase kinase; PKA, cAMP-dependent protein kinase; TPK, tyrosine-specific protein kinase; v-Fps, nonreceptor TPK and transforming agent of the Fujinami sarcoma virus.

10.1021/bi001216g CCC: $19.00
Published on Web 10/04/2000

Scheme 1

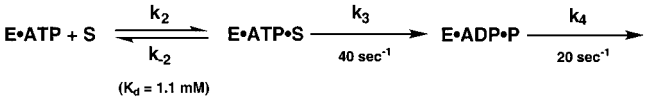

of the GRL of PKA to cleavage agents suggesting that this crystallographic phenomenon may have relevance in a solution setting (*9*). The GRL of the InRK moves upon ATP binding and "activation" loop phosphorylation, an essential, activating event (*4*, *10*). The "activation" loop does not directly contact the GRL but does influence the position of active-site residues, a nearby α helix and the orientation of the domains. In the inactive form of this enzyme (nonphosphorylated "activation" loop), the GRL appears to be sterically impairing the closure of the two domains of the kinase core. These movements in PKA and the InRK suggest that the GRL of protein kinases may serve as a "clamp" or "lid" for ATP, improving affinity, enhancing phosphoryl group donation to a protein or peptide substrate and limiting unproductive phosphorylation of water (ATPase).

The application of site-directed mutagenesis has provided some exciting insights into the function of the GRL of PKA. Substitution of the second glycine in the loop lowers the rate of the phosphoryl transfer step by more than 2 orders of magnitude while replacement of the first and third glycines have more modest effects (*6*). All three glycines are important for ATP binding although the second glycine does not significantly impact ADP binding (*6*). These results indicate that Gly-52 is important for selectively enhancing the affinity of ATP without influencing the affinity of the product nucleotide. A differential effect of this type can be viewed as beneficial since it maintains quick release of ADP without destabilizing ATP, an outcome that would otherwise lead to reduced phosphoryl transfer to peptide substrates (*6*). In this manner, the GRL of PKA accommodates ATP, locks the triphosphoryl region for committed protein phosphorylation and then utilizes its inherent flexibility to expel ADP. This compelling model for the role of the GRL in PKA could have some general applications to other protein kinases given the close structural relationship of the enzymes in this family and the highly conserved utilization of glycine residues.

To determine whether the GRL possesses common functional characteristics, we replaced the conserved glycines in the loop of the oncoprotein, v-Fps, with serine and alanine residues and measured the effects of these single-site substitutions on the catalytic mechanism of the enzyme. These studies were performed on v-Fps for several reasons. First, the catalytic portion of v-Fps is a tyrosine protein kinase (TPK) so that it offers an interesting comparison with the serine-specific kinase domain of PKA. Second, the active kinase domain of v-Fps can be expressed at suitable levels using a bacterial expression system for detailed kinetic analyses (*11*). Third, a sufficient understanding of the kinetic mechanism for the wild-type kinase domain of v-Fps exists, providing a good background for comparative studies (*12*−*14*). The results from steady-state kinetic, inhibition, and viscosometric studies have been used to establish the wild-type kinetic mechanism shown in Scheme 1.

At high ATP concentrations, v-Fps binds nine residue peptides (e.g., S = EAEIYEAIE) with moderate affinity. The rate of peptide phosphorylation is slow compared to that observed in PKA (500 vs 40 s^{-1}). This leads to a v-Fps mechanism in which net product release is partially rate limiting, but it is unclear whether ADP or phosphopeptide dissociation or a conformational change limits this step. Nonetheless, the utility of this kinetic pathway has been realized in the analyses of mutant forms of the enzyme where the function of specific residues on kinase activation and substrate specificity have been established (*15*, *16*).

The TPK family of enzymes is distinguished from other protein kinases partly by its substrate specificity but also by its localization, structural complexity, and function in the cell. The TPKs are usually placed into two general classifications: receptor and nonreceptor TPKs. The former are integral membrane proteins and possess extracellular and intracellular domains separated by a short membrane spanning segment. The intracellular domain contains the kinase domain and the extracellular domain contains a variety of subdomains important for recognizing signaling molecules. The nonreceptor TPKs may be peripherally bound to the membrane or may be cytoplasmic in location but migrate to the membrane upon receptor TPK signaling. v-Fps is a nonreceptor TPK, and as a member of the Fps/Fes subfamily, its cellular forms are predominantly expressed in hematopoietic cells. It has been shown that the Fps/Fes enzymes are essential for the terminal differentiation of macrophages (*17*, *18*) but oncogenic forms cause cardiac and neurological disorders in mice (*19*, *20*). The Fps/Fes families are complex proteins with molecular masses in excess of 90 kDa and are composed of noncatalytic domains that regulate the function of the kinase domain in the absence of receptor signaling. The SH2 domains of Fps/Fes enzymes are important for protein−protein interactions (*21*−*23*). v-Fps differs from its cellular forms by the addition of a retroviral gag sequence at the N-terminus which imparts membrane association (*24*) and could provide the origin for the transforming potential of this oncoprotein. In this present study, we have demonstrated through detailed kinetic studies that the GRL of this oncoprotein (I_{927}GRGNFGEV) is not only important for controlling the rate of phosphoryl transfer but it also controls the relative affinities of ATP and ADP, an important effect needed for high ATP affinity and rapid release of ADP.

MATERIALS AND METHODS

Materials. Adenosine 5′-triphosphate (ATP), phosphoenolpyruvate, magnesium chloride, nicotinamide adenine dinucleotide, reduced (NADH), isopropyl-β-thiogalactoside (IPTG), tris(hydroxymethyl)aminomethane (Tris), 3-(*N*-morpholino) propane sulfonic acid (Mops), pyruvate kinase, type II, from rabbit muscle, lactate dehydrogenase, type II, from bovine heart and ethylenediamine tetraacetic acid (EDTA) were purchased from Sigma. Dithiothreitol (DTT) was purchased from Fisher. Media supplies (yeast extract and tryptone) were purchased from Difco. Oligonucleotides were synthesized by Retrogen. DNA mini-prep kits were purchased from Qiagen. The plasmid vector pGEX-2T was purchased from Pharmacia. *E. coli* strain BL21(DE3) was purchased from Novagen. QuikChange and *E. coli* strains, XL1-Blue and SURE, were purchased from Stratagene.

Construction of the GRL Mutant Proteins. Mutants in the kinase domain of the v-Fps gene were made by PCR using the Stratagene Quik-Change kit and an MJ Research PCT

200 Peltier Thermocycler. Two overlapping oligonucleotides are required to create the desired mutation. The following pairs of oligonucleotides were used to make the mutations: $G928^{A}_{S}$, 5′-GGGGAGCGCATT$^{GCC}_{AGC}$CGGGGGAACTTC-3′ and 5′-GAAGTTCCCCCG$^{GGC}_{GCT}$AATGCGCTCCCC-3′; $G930^{A}_{S}$, 5′-GCATTGGCCGG$^{GCC}_{AGC}$AACTTCGGGGAG-3′ and 5′-CTCCCCGAAGTT$^{GGC}_{GCT}$CCGGCCAATGCG-3′; $G933^{A}_{S}$, 5′-GGGAACTTC$^{GCC}_{AGC}$GAGGTGTTCAGCGGC-3′ and 5′-GCCGCTGAACACCTC$^{GGC}_{GCT}$GAAGTTCCC-3′. The PCR reactions were performed in a total volume of 50 μL with 60 mM Tris (pH 9.1), 18 mM $(NH_4)_2SO_4$, 1.8 mM $MgSO_4$, 5−50 ng of template DNA, 0.2 mM of each dNTP, 2.5 units of *PFUTurbo* DNA Polymerase and 125 ng of each primer. The PCR cycle created the mutation in the gene while amplifying the plasmid and gene together. The plasmid was purified and transformed into *E. coli* strain, XL1-Blue, or a recombinant minus *E. coli* strain, SURE. Several clones were selected and their entire kinase genes sequenced. The mutant plasmids with the correct sequence were then transformed into *E. coli* strain BL21(DE3) and expression of the GST fusion protein was confirmed on a 13% polyacrylamide gel.

Peptides and Protein Purification. Substrate peptide, EAEIYEAIE, was synthesized by the USC Microchemical Core Facility using Fmoc chemistry and purified by C-18 reversed-phase HPLC. The concentrations of the peptides were determined by weight. BL21(DE3) cells containing the mutant or wild-type plasmids were grown to an OD^{600} of approximately 0.5−0.8 at 37 °C in 2−6 L of LB media and induced for 3 h with 0.5 mM IPTG at 24 °C. The cells were harvested by centrifugation in a Sorvall GS3 rotor at 6000 rpm for 5 min at 4 °C. The wild-type and mutant fusion proteins, GST-kin, were purified using a glutathione agarose affinity resin according to previously published procedures (*11*). The total concentration of the protein was determined by a Bradford assay (approximately 3−4 mg for wild-type and mutant proteins) and the concentration of the fusion protein (M_r 58 000) was determined by gel densitometry (*15, 16*). The enzyme was stored at −70 °C in a buffer containing 50 mM Tris (pH 7.5), 1 mM EDTA, 150 mM NaCl, 1 mM DTT, 10% glycerol. The enzyme was thawed on ice (4 °C) and used immediately for each kinetic study.

Autophosphorylation of Wild-Type and Mutant Proteins. Affinity-purified wild-type and mutant forms of GST-kin (6.3−48 μg) were mixed with 2−5 μL of [^{32}P γ]ATP in a final volume of 50 μL of 0.1 M Mops (pH 7) and 12 mM $MgCl_2$. After 12−24 h of incubation time at 25 °C, 50 μL of SDS−PAGE loading dye was added to stop the reaction. The mixture was boiled for 2−5 min and run on a 10% SDS−PAGE gel. The gel was stained, destained, and air-dried. The dried gel was then exposed for 1−5 min at 25 °C using Kodak's Biomax film.

Kinetic Assay. The enzymatic activities of wild-type and mutant forms of GST-kin were measured spectrophotometrically using a coupled enzyme assay. This assay couples the production of ADP with the oxidation of NADH using pyruvate kinase and lactate dehydrogenase. Typically, substrate peptide (0.1−2.5 mM) was mixed manually with ATP (0.02−2.5 mM), $MgCl_2$ (10−12.5 mM), and GST-kin (17−690 nM) in a 50 μL (minimum volume) quartz cuvette containing 0.40 mM phosphoenolpyruvate, 0.20 mM NADH, 2 units of lactate dehydrogenase, and 0.5 units of pyruvate kinase. The total concentration of $MgCl_2$ needed to obtain a desired, free concentration of Mg^{2+} was calculated based on the dissociation constants of 0.0143 mM for Mg-ATP, 5 mM for Mg-PEP, and 19.5 mM for Mg-NADH (*25*). All reactions were measured in a Beckman DU640 spectrophotometer equipped with a microcuvette holder in a buffer containing 100 mM Mops at pH 7.0, in a final volume of 60 μL at 24 °C. Background reactions in the absence of substrate peptide were performed to correct for ATPase activity which did not exceed 10% of the substrate-dependent reaction for wild-type or mutant enzymes. Absorbance changes at 340 nm were collected over a time range of 100−170 s. Less than 10% of the substrate peptide was consumed in each initial velocity measurement. All initial velocities varied linearly with the concentration of the fusion protein.

Measurement of the K_I Values for ADP. The K_I values for ADP were measured using a radiochemical assay similar to a previously published protocol (*11*). Wild-type and mutant forms of GST-kin (6.3−48 μg) were preequilibrated with substrate peptide (3 mM), 10 mM free Mg^{2+}, and varying amounts of ADP (0.062−6.8 mM) and the reactions were started with [^{32}P γ]ATP (0.058−0.14 mM, 82 200 cpm/mmol). The reactions (40 μL final volume) were stopped after 2 min using 300 μL of 30% acetic acid. The quenched reaction was then applied to a polypropylene column containing 2 mL of DE-52 resin preequilibrated with 30% acetic acid. After absorption, the phosphorylated peptide was washed through the column using 5 mL of 30% acetic acid, collected directly into scintillation vials, mixed with scintillation fluid and counted. Control experiments were performed by running the above reaction without enzyme. The background CPMs were normally less than 5% of the experimental values. The specific activity of [^{32}P-γ]ATP was determined by diluting a portion of the reaction mix 300-fold.

Viscosometric Measurements. The relative solution viscosities (η^{rel}) of buffers containing sucrose were measured relative to a standard buffer of 100 mM Mops, pH 7.0, at 23 °C, using an Ostwald viscometer (*26*). Each viscosity measurement was carried out using 5.0 mL of buffer containing varying amounts of viscosogen. The amount of time required for each buffer to move through the markings on the viscometer was recorded. The relative viscosity of each buffer was calculated using eq 1:

$$\eta^{rel} = \frac{t\,(\%)}{t} \times \frac{\rho\,(\%)}{\rho} \qquad (1)$$

where η^{rel} is the relative solvent viscosity, t (%) and t are the transit times for a given viscous buffer and the standard buffer, respectively, and ρ (%) and ρ are the densities of the viscous and standard buffers, respectively. The following relative solvent viscosities were obtained for the buffers (% viscosogen, η^{rel}): 33% sucrose, 3.4; 26% sucrose, 2.1; 20% sucrose, 1.7.

Molecular Modeling. A structural model of the kinase domain of v-Fps was generated with the programs Homology and InsightII (MSI, 2000) using as a template the crystallographic coordinates of the InRK (1ir3 in pdb database). This template was cocrystallized with a peptide substrate and an ATP analogue (AMP-PCP) and represents the trisphosphorylated, fully activated form of the kinase (*4*). After

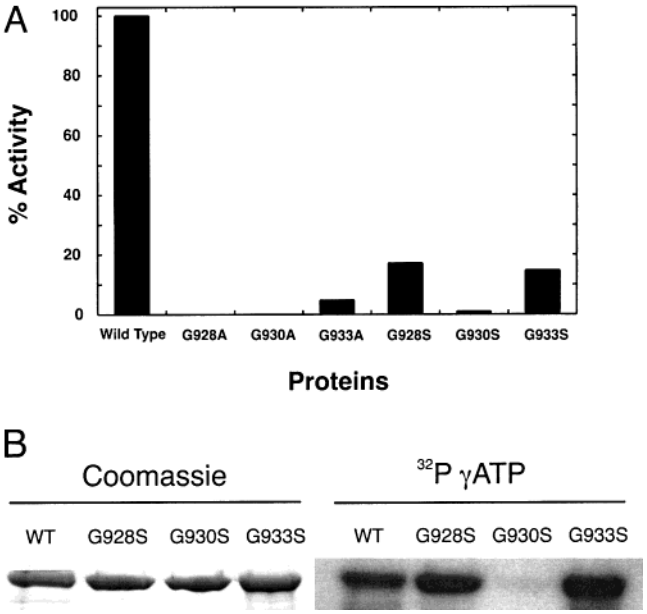

FIGURE 1: Biophysical properties of wild-type and GRL mutants of v-Fps. (A) The relative specific activities of wild-type and mutant proteins. The activities of the proteins are measured using 3 mM ATP, 13 mM $MgCl_2$, and 0.5 mM EAEIYEAIE in 100 mM Mops (pH 7) and the protein concentrations are measured using a Bradford assay. The specific activities of the mutants are displayed relative to wild-type which is set at 100%. (B) Autophosphorylation of wild-type and the glycine-to-serine mutants. The proteins were pre-equilibrated with [^{32}P γ]ATP and run on a 10% polyacrylamide gel. Each lane contains approximately 8−10 μg of protein. The coomassie stain of the gel is shown on the left whereas the autoradiogram of this gel is displayed on the right.

homology modeling, the structure of v-Fps kinase was energy minimized for 10 000 iterations using distance-dependent dielectric constants with the program Discover (MSI, 2000).

Kinetic Data Analysis. The steady-state kinetic parameters V_{max}, $K_{peptide}$, and K_{ATP} were obtained by plotting the initial reaction velocity versus the total substrate concentration at fixed ATP or the total ATP concentration at fixed peptide using the Michaelis−Menten equation. The maximum reaction velocity (V_{max}) was converted to k_{cat} by dividing V_{max} by the total enzyme concentration.

RESULTS

Specific Activities and Autophosphorylation of Mutant Enzymes. To evaluate the catalytic properties of the mutants, specific activities were measured using 3 mM ATP, 0.5 mM substrate peptide and 13 mM $MgCl_2$. Figure 1A shows the relative specific activities of the proteins compared to wild-type (100%). While no activity was detected for G928A and G930A, the other mutants exhibited low and varying activities. Based on the detection limits of the spectrophotometric assay, if G928A and G930A were active they would possess less than 0.1% of the wild-type specific activity. To determine whether the mutant proteins were capable of autophosphorylating, the ability of wild-type and mutants to incorporate ^{32}P was monitored. Equivalent amounts of the wild-type and the serine mutants were preequilibrated with identical amounts of [^{32}P γ]ATP. The enzyme samples were then run on a 10% polyacrylamide gel and exposed for approximately 2 min. Figure 1B shows the commassie-stained gel and autoradiogram for wild-type along with the mutants. G928S and G933S incorporated phosphate at levels comparable to the wild-type enzyme while G930S incorporated very little phosphate over the same incubation time. The faint band for G930S is more prominent at longer gel exposure times (data not shown) indicating that this mutant is autophosphorylated but this posttranslational modification occurs at a reduced level. G928A and G930A do not incorporate noticeable amounts of ^{32}P at exposure times where G933A and wild-type are autophosphorylated (data not shown). It has been demonstrated that the kinase domain of v-Fps is phosphorylated uniquely at Tyr-1073 in both eucaryotic and bacterial expression systems at a stoichiometry of approximately 0.6 phosphates/enzyme (*27*, *28*). On the basis of this level of incorporation, G928S and G933S are phosphorylated at a similar level while G930S is estimated to incorporate less than 0.03 phosphates/enzyme. In a separate experiment, we demonstrated that the incorporation of radiolabeled phosphate into the proteins is not the result of phosphorylation of the fusion component, GST. Cleavage of wild-type and the serine mutants with thrombin did not produce a radiolabeled GST band on a polyacrylamide gel (data not shown).

Table 1: Steady-State Kinetic Parameters for the Mutant Forms of v-Fps[a]

protein	k_{cat} (s^{-1})[b]	K_{ATP} (μM)[c]	$K_{peptide}$ (μM)[b]	K_I^{ADP} (μM)[d]
wild-type	14 ± 3	220 ± 30	400 ± 100	370 ± 45
G928S	4.4 ± 0.40	120 ± 16	1600 ± 150	700 ± 200
G930S	0.31 ± 0.04[e]	1000 ± 150	1200 ± 230	1000 ± 100
G933S	2.3 ± 0.21	42 ± 10	500 ± 150	17 ± 2
G933A	0.66 ± 0.07	60 ± 6	250 ± 10	53 ± 5

[a] The kinetic parameters, k_{cat}, K_{ATP}, and $K_{peptide}$, were measured in 100 mM Mops (pH 7) buffer at 23 °C using a spectrophotometric assay. [b] k_{cat} and $K_{peptide}$ were measured using 3 mM ATP and 13 mM $MgCl_2$ and varying peptide concentrations (0.01−2.5 mM). [c] K_{ATP} was measured using fixed concentrations of peptide (2.5 mM) and 10 mM free Mg^{2+} and varying ATP concentrations (0.025−2.5 mM). [d] This parameter was measured using a radiochemical assay. [e] k_{cat} was corrected for the experimental concentration of ATP (3 mM) using the Michaelis−Menten equation.

Steady-State Kinetic and Inhibition Studies. The steady-state kinetic parameters of the mutants and wild-type were measured under conditions of variable substrate peptide (0.01−2.5 mM), EAEIYEAIE, and fixed ATP (3 mM) or variable ATP (0.025−2.5 mM) and fixed substrate peptide (2.5 mM). Under all conditions, the concentration of the free Mg^{2+} was kept constant at 10 mM. Since no activity was detected for G928A and G930A at the highest concentrations of peptide (2.5 mM) and ATP (3 mM) only G933A and the serine mutants were studied. The steady-state kinetic parameters for these mutants are displayed along with wild-type enzyme in Table 1. In general, the mutants lower turnover (k_{cat}) by 3−45-fold while K_{ATP} is either increased or decreased by as much as 5-fold. $K_{peptide}$ is increased by as much as 4-fold or decreased by as much as 2-fold. In plots of initial velocity versus ATP concentration, the apparent K_{ATP} (K_{ATP}^{app}) was increased in the presence of ADP without affecting k_{cat}, indicating that ADP is a competitive inhibitor of wild-type v-Fps (data not shown). The inhibitory constants for wild-type and the mutants were then measured using a competitive Dixon plot (*29*). The apparent K_I values are

Table 2: Effects of Solvent Viscosity on the Kinetic Parameters of Mutant Forms of v-Fps[a]

protein	wild-type[b]	G928S	G930S	G933S	G933A
$(k_{cat})^{\eta}$	0.63	0.06[c]	0.01[c]	0.64 ± 0.08	0.60 + 0.05
$(k_{cat}/K_{peptide})^{\eta}$	0	−0.08[c]	−0.15[c]	−0.09 ± 0.010	
$(k_{cat}/K_{ATP})^{\eta}$	0				0.09 ± 0.15
K_d (mM) ATP[d]	0.60	0.12	1.0	0.12	0.10
K_d (mM) peptide[d]	1.1	1.6	1.2	0.73	0.74
k_3 (s^{-1})[e]	40	4.4	0.3	6.4	1.6
k_4 (s^{-1})[e]	20	fast	fast	3.6	1.1

[a] All kinetic parameters were measured in 100 mM Mops (pH 7) buffer at 23 °C using 10 mM free Mg^{2+}. [b] These data were taken from refs *12*−*14*. [c] These slope values are based on steady-state kinetic parameters measured at 0 and 33% sucrose. [d] The K_d values were measured using eq 5. [e] The values of k_3 and k_4 were derived from the expression for the turnover number $[k_3k_4/(k_3+k_4)]$ and $(k_{cat})^{\eta}$ by the following relationships: $k_4 = k_{cat}/(k_{cat})^{\eta}$ and $k_3 = k_{cat}/[1 - (k_{cat})^{\eta}]$.

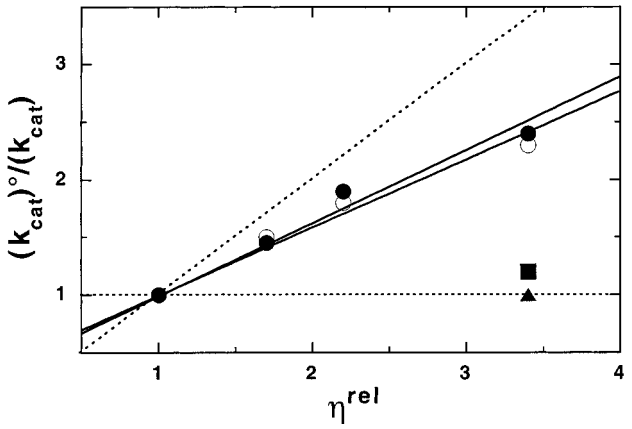

FIGURE 2: Effects of solvent viscosity on k_{cat} for G928S (■), G930S (▲), G933S (●), and G933A (○). $(k_{cat})°/k_{cat}$ is the ratio of k_{cat} in the absence and presence of varying percent of sucrose and η^{rel} is the relative solvent viscosity. The data for G933S and G933A were fit to linear functions and the slope values are reported in Table 2. The dotted lines represent slopes of 1 (where the *y*-intercept is the origin) or 0 (where the *y*-intercept is the 1).

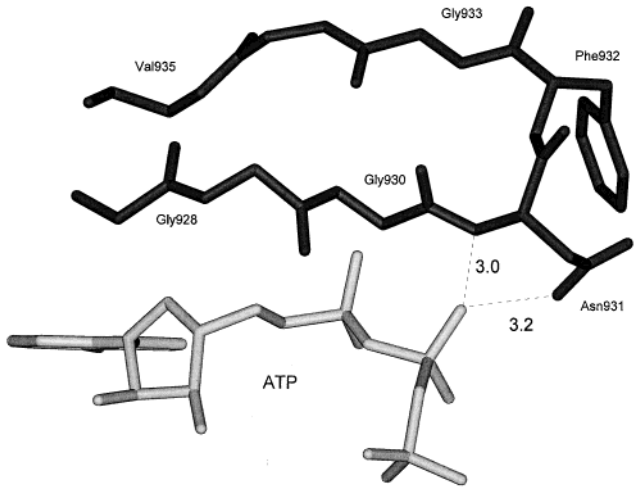

FIGURE 3: Molecular model of the GRL of v-Fps based on the crystallographic coordinates of the InRK (*4*). The backbone residues from position 928−935 and the side chains of Phe-932, Asn-931, and Val-935 are displayed. The distances between the amino backbone and side chain nitrogens of Asn-931 are shown in units of angstroms.

corrected for the concentration of ATP and the true K_I values are displayed in Table 1.

Viscosity Effects on Kinetic Parameters. The influence of sucrose on the steady-state kinetic parameters, k_{cat}, $k_{cat}/K_{peptide}$, and k_{cat}/K_{ATP}, was measured for the mutant enzymes. The initial velocities of the enzyme reactions were monitored either as a function of peptide concentration (0.1−2.5 mM) at fixed ATP (3 mM) or as a function of ATP concentration (0.02−2.5 mM) at fixed substrate peptide (2.5 mM) under conditions of varying percentages of sucrose. For all velocity measurements, the concentration of free Mg^{2+} was fixed at 10 mM by varying the total amount of $MgCl_2$. The ratios of the steady-state kinetic parameters, k_{cat}, $k_{cat}/K_{peptide}$ and k_{cat}/K_{ATP}, in the absence and presence of sucrose $[(k_{cat})°/k_{cat}$, $(k_{cat}/K_{peptide})°/(k_{cat}/K_{peptide})$, and $(k_{cat}/K_{ATP})°/(k_{cat}/K_{ATP})]$ were measured as a function of relative viscosity (η^{rel}). A plot of $(k_{cat})°/k_{cat}$ as a function of η^{rel} for G933S and G930A is shown in Figure 2. All data were fit to linear functions and the slope values $[(k_{cat})^{\eta}$, $(k_{cat}/K_{peptide})^{\eta}$ and $(k_{cat}/K_{ATP})^{\eta}]$ are listed in Table 2. For G928S and G930S, the presence of 33% sucrose did not significantly alter k_{cat} or $k_{cat}/K_{peptide}$. For G928S, $(k_{cat})°/k_{cat}$ and $(k_{cat}/K_{peptide})°/(k_{cat}/K_{peptide})$ are 1.1 ± 0.22 and 0.8 ± 0.20, respectively. For G930S, $(k_{cat})°/k_{cat}$ and $(k_{cat}/K_{peptide})°/(k_{cat}/K_{peptide})$ are 1.1 ± 0.22 and 0.7 ± 0.20, respectively. Since high sucrose did not significantly affect these parameters, a complete series of viscous agents were not examined. The effects of high sucrose on k_{cat} for these two mutants are shown in Figure 2 as single points. Slope estimates were derived from these points using the data point at $\eta^{rel} = 1$, $(k_{cat})°/k_{cat} = 1$ and are displayed in Table 2. At the highest sucrose concentration (33%), the observed reaction velocities are enzyme dependent indicating that any rate reductions compared to 0% sucrose are not due to inhibition of the coupling agents.

Molecular Model of the GRL of v-Fps. Figure 3 shows a stick model of the GRL of v-Fps (residues 928−935) derived from molecular modeling studies using the crystallographic coordinates for the InRK. Only the side chains of residues Asn-931, Phe-932, and Val-935 are shown for clarity. While Phe-932 does not contact ATP, Val-935 stacks onto the adenine ring, an interaction that is conserved in both the InRK and PKA. The side chain amido nitrogen and the backbone nitrogen of Asn-931 make close contacts with β phosphate of ATP. This residue occupies the same position as Ser-1006 in the InRK although the side chain in this TPK does not contact ATP (*4*). In contrast, a serine is also present in this position in the GRL of PKA (Ser-53) but it contacts the axial oxygen of the γ phosphate rather than the β phosphate (*2*). This model suggests that the GRL of v-Fps may make a unique contact with ATP that is not observed in either PKA or InRK.

DISCUSSION

Mutational Tolerance in the GRL. Six mutations were inserted in three conserved glycine residues of the GRL using

site-directed mutagenesis. The viability of the resulting mutants were assessed initially by their abilities to phosphorylate an exogenous substrate peptide (EAEIYEAIE) and to autophosphorylate within the kinase domain. While all three serine substitutions are well tolerated, only one of the three alanine replacements (G933A) produces an enzyme with measurable activity (Figure 1A). This result is somewhat consistent with the level of sequence conservation observed throughout the protein kinase family. The third glycine of the GRL exhibits the highest level (15%) of variability (*1*) and, in the context of these mutagenesis studies, demonstrates a broader tolerance for other residues than do the first and second glycines. There is also a noticeable correlation between the turnover numbers of the mutants and their abilities to incorporate phosphate into the kinase domain. v-Fps has a site in the "activation" loop of the kinase domain (Tyr-1073) that is uniquely autophosphorylated in bacterial and eucaryotic expression systems at a stoichiometry of approximately 0.6 phosphates/enzyme (*11*, *22*). Comparing the glycine-to-serine substitutions, G928S and G933S incorporate phosphate into the kinase domains at similar levels as wild-type (Figure 1B) while G930S shows less than 5% incorporation compared to wild-type. Accordingly, the turnover number of G930S is lower than those of G928S and G933S (Table 1). The poor autophosphorylation for G930S is a manifestation of the importance of this glycine for generating an active enzyme form. Underphosphorylation may have compound effects owing to changes in the GRL and the "activation" loop which contains the phosphorylation site. Nonetheless, as will be demonstrated in the next two sections, this potential complexity is not evident in changes in nucleotide or substrate affinity.

Application of Viscosity Methods to Protein Kinase Mutants. It has been demonstrated for several protein kinases that the steady-state kinetic parameters do not routinely reflect singular events in the catalytic mechanism. For instance, k_{cat} in v-Fps does *not* uniquely reflect either the phosphoryl transfer or the product release step (Scheme 1). Also, $K_{peptide}$ for v-Fps is 3-fold lower than the dissociation constant (K_d) owing to the relative values of k_3 and k_4 (vide infra). For PKA, K_d is approximately 20-fold higher than $K_{peptide}$ further complicating the interpretation of the steady-state kinetic values (*30*). These problems have serious implications for the interpretation of mutations in protein kinases. In two examples, mutations in the autophosphorylation sites of PKA and v-Fps cause increases in $K_{peptide}$ without affecting the K_d for the substrate (*16*, *31*). The inability to differentiate between true and apparent substrate affinities in these two cases would lead to incorrect assessments regarding the role of the phosphorylation sites and the function of the loop segments containing them. Indeed, the advised approach toward understanding protein kinase function on a molecular scale is to integrate the kinetic results of mutations into a detailed wild-type kinetic mechanism (Scheme 1). The application of the viscosity method toward this goal has been essential for the interpretation of mutations in several protein kinases including v-Fps (*15*, *16*), PKA (*6*, *31*, *32*), phosphorylase kinase (*33*), and Csk (*34*−*36*).

The viscosity data in Figure 2 and Table 2 can be evaluated according to the three-step mechanism presented in Scheme 1. By applying the Stokes−Einstein relationship which equates diffusion coefficients and intrinsic viscosity, a direct correlation between the steady-state kinetic parameters, k_{cat} and $k_{cat}/K_{peptide}$, and the relative solvent viscosity of the medium can be made (Table 2). Plots of either kinetic parameter as a ratio in the absence and presence of viscosogen versus relative solvent viscosity are linear (Figure 2) and the slope values conform to eqs 2 and 3:

$$(k_{cat})^{\eta} = \frac{k_3}{k_3 + k_4} \tag{2}$$

$$(k_{cat}/K_{peptide})^{\eta} = \frac{k_3}{k_{-2} + k_3} \tag{3}$$

A relationship describing the effects of viscosogens on k_{cat}/K_{ATP} can also be derived under conditions of high substrate concentration assuming that the first step in Scheme 1 now corresponds to ATP binding and bears the forward and reverse rate constants, k_1 and k_{-1}. This relationship is shown in eq 4.

$$(k_{cat}/K_{ATP})^{\eta} = \frac{k_3}{k_{-1} + k_3} \tag{4}$$

Equations 2−4 predict that the slope values will fall between the limits of 0 and 1 where the former represents a viscosity-insensitive parameter and the latter represents a viscosity-sensitive parameter. As shown in Table 2, these slope values conform to these limits, but, in some cases, the slope values are slightly negative. Since these values are small, we consider them as zero in our data interpretation.

We can use the rate expressions for k_{cat} $[k_3k_4/(k_3 + k_4)]$, $k_{cat}/K_{peptide}$ $[k_2k_3/(k_{-2} + k_3)]$, and k_{cat}/K_{ATP} $[k_1k_3/(k_{-1} + k_3)]$ and eqs 2−4 to determine the individual steps in Scheme 1. Since ATP and peptide exchange rapidly with the enzymes (i.e., no effects of viscosity on $k_{cat}/K_{peptide}$ or k_{cat}/K_{ATP}), the individual rate constants, k_1, k_{-1}, k_2, and k_{-2}, are indeterminate but the dissociation constants for ATP and the substrate peptide can be assessed using eq 5,

$$K_d = \frac{K_m}{[1 - (k_{cat})^{\eta}]} \tag{5}$$

where K_m represents either K_{ATP} or $K_{peptide}$. By applying this approach to wild-type v-Fps and the mutants, the individual steps in the kinetic mechanism can be assigned (Table 2). Although we have not measured $(k_{cat}/K_{ATP})^{\eta}$ for all the enzymes, it is reasonable to presume that this term will be near zero in all cases. G933A and G933S are very similar with respect to their steady-state kinetic parameters, and as we will see in the next several sections, this similarity extends to the individual steps in the kinetic mechanism. Also, the k_{cat} values for all mutants are lower than wild-type, an effect that retains the rapid equilibrium mechanism for the substrate (Scheme 1).

Effects of Mutations on the Phosphoryl Transfer Step. The effects of serine substitution on the glycines of the GRL have significant impact on the rates of phosphoryl transfer (Table 2). While G928S and G933S have values of k_3 that are 6- and 9-fold lower than that for wild-type, replacement of the central glycine with serine (G930S) lowers this step by 130-fold. On the basis of these results, Gly-930 is certainly the most important glycine of the GRL for generating an enzyme

form that adequately stabilizes the phosphoryl transfer transition state. However, interpretation of the effects of GRL substitutions must take into account the phosphorylation states of the mutants. While serine mutations at Gly-928 and Gly-933 are directly comparable with the wild-type enzyme since they are phosphorylated to similar extents (Figure 1), the rate reduction in k_3 for G930S is likely the result of double effects of the GRL replacement and activation loop dephosphorylation. In a previous study, it was shown that dephosphorylation of the activation loop results in a decrease in k_3 of 140-fold based on the kinetic evaluation of a mutant enzyme form of v-Fps, Y1073F (*16*). This decrease in the rate of phosphoryl group transfer is similar to that observed for G930S (Table 2). For PKA, the phosphoryl transfer rate in T197A, the activation loop mutant that mimics the dephosphorylated state, is the same as that for the isoform of G52S that lacks Thr-197 phosphorylation (*5*, *31*). This outcome is identical to that for v-Fps and may suggest similar synergistic effects between the two loops in both protein kinases. Whether the central glycine in the GRLs of these two protein kinases serve similar functions in the activated enzyme is still unknown. Although an X-ray structure for v-Fps is currently unavailable, the molecular model in Figure 3 identifies two unique contacts with Asn-931 and the β-phosphate of ATP. Substitution of the adjacent glycine at position 930 may have the largest effect among the glycine replacements on k_3 and autophosphorylation owing to its proximity to this residue. Replacing the glycines at positions 928 and 933 may be better accepted if they do not affect Asn-931.

Glycine Substitution Does Not Influence Substrate Binding. Although G928S and G930S increase $K_{peptide}$ by 4- and 3-fold compared to wild-type (Table 1), neither mutation alters the true affinity of the peptide (Table 2). This outcome can be understood in light of eq 5 which can be rearranged to relate $K_{peptide}$ with the individual steps in Scheme 1 [$K_d k_4/(k_3 + k_4) = K_{peptide}$]. The observed increase in $K_{peptide}$ for G928S and G930S is not due to changes in K_d but rather is due to changes in the kinetic mechanism. When $k_3 > k_4$ (wild-type case), the true affinity of the peptide is lower than that judged by the apparent affinity constant (i.e., $K_d > K_{peptide}$). Alternatively, when $k_4 > k_3$ (rate-limiting phosphoryl transfer; G928S and G930S cases), the true and apparent affinities of the peptide are identical. For G933S and G933A, $K_{peptide}$ is either unchanged or about 2-fold lower than that for wild-type (Table 1). Surprisingly, the K_ds for these mutants are approximately 2-fold higher than wild-type, an apparent reversal in effects on K_d and $K_{peptide}$. This phenomenon can be explained since the rate of phosphoryl transfer in these mutants is still fast relative to net product release ($k_3 > k_4$). Nonetheless, the changes in K_d for the peptide are still small for the mutants and unaffected for replacements in the first and second glycines. These results indicate that the glycines of the GRL do not directly or indirectly influence the substrate pocket. In comparison, replacement of any of the three glycines in the GRL of PKA reduces the affinity of the substrate peptide by 10-fold (*6*). It is not clear why this occurs but certainly there are differences in how the GRLs of these two kinases influence substrate recognition.

Product Release and the GRL. The development of a kinetic mechanism using viscosometric methods relies upon the partitioning of viscosity-sensitive and -insensitive steps.

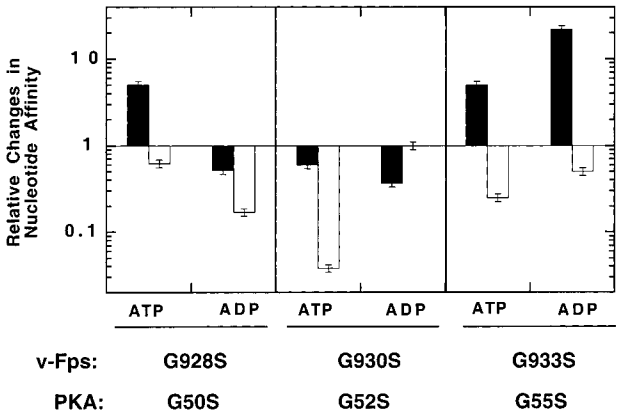

FIGURE 4: Changes in ATP and ADP affinities for the three glycine-to-serine substitutions in the GRLs of v-Fps (filled bars) and PKA (open bars) compared to wild-type. The *y*-axis represents the ratios of K_d for ATP or K_I for ADP for wild-type and mutant enzymes. A value greater than 1 on the *y*-axis represents an improvement in nucleotide affinity for the mutant compared to wild-type whereas a value less than 1 indicates reduced affinity compared to wild-type. The data for v-Fps are taken from Tables 1 and 2 and that for PKA are taken from (*6*).

While control experiments were performed to demonstrate that the phosphoryl transfer step in the wild-type enzyme is not affected by added viscosogens (*12*), it is not straightforward to assign the viscosity-dependent release step in Scheme 1. Problems arise because the kinase reaction produces two products and it is unclear which product, either ADP or phosphopeptide, limits k_4. Furthermore, conformational changes can be sensitive to solvent viscosity (*37*), making the identification of k_4 more uncertain. While it is unknown which step or steps limit net product release for wild-type v-Fps, the GRL mutants may provide some insights into this dilemma. For G933S and G933A, discrete values for k_4, which are 6- and 18-fold *lower* than that for wild-type, can be measured (Table 2). These reductions in net product release are accompanied by 22- and 7-fold *decreases* in K_I for one of the products, ADP, for G933S and G933A (Table 1). If the mutations do not influence the association rate constant for ADP, then we anticipate a direct correlation between the enhanced affinities and reduced dissociation rate constants for ADP. The similar magnitudes for the decreases in k_4 and K_I for ADP could mean that the release of this product is partially rate limiting in k_{cat} for the two mutants. This proposal does not imply, of course, that ADP release is rate limiting for k_4 in the wild-type enzyme but these correlations between K_I and k_4 offer a compelling role for the GRL. The presence of glycine residues in the GRL may enhance the flexibility of the loop so that it can serve as an effective "lid" for the nucleotide-binding pocket. The GRL may confer enough flexibility such that ATP can enter and ADP can exit with minimal resistance. In the productive ternary complex (E·ATP·S), the GRL may cover the triphosphate region of ATP, facilitate phosphoryl transfer to substrates as evidenced by the reductions in this step upon mutation, and then shift its conformation so that ADP can quickly dissociate.

Nucleotide Specificity and the GRL. By using viscosity and inhibition studies, the affinities of the mutants for ATP and ADP can be evaluated (Tables 1 and 2). Figure 4 displays the effects of the three serine replacements on nucleotide binding compared to wild-type v-Fps (solid bars). The first

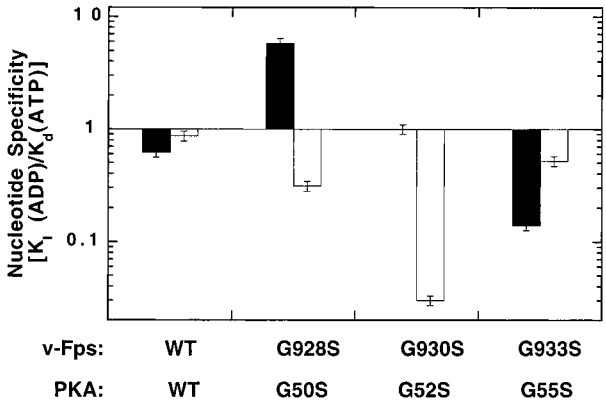

FIGURE 5: Preference of wild-type and GRL mutant forms of v-Fps (filled bars) and PKA (open bars) for binding ATP compared to ADP. Values greater than 1 on the *y*-axis indicate that the enzyme prefers to bind ATP over ADP whereas values less than 1 indicate that the enzyme prefers to bind ADP over ATP. The data for v-Fps are taken from Tables 1 and 2 and that for PKA are taken from (*6*).

(G928S) and third (G933S) mutations in the GRL of v-Fps actually improve the affinity of ATP while the second (G930S) replacement has a small negative effect on binding. In comparison, the first and second replacements mildly weaken ADP affinity while the third replacement improves affinity by 22-fold. If one of the functions of the GRL is to enhance the rate of nucleotide binding, it is reasonable to expect that this acceleration may come at the cost of higher nucleotide affinity. Higher affinity may involve more contacts between the nucleotide and active site and, if some of these additional interactions are induced or occlude the binding pocket, net association may be impaired. This could explain why the replacement of some of the glycines increases the affinity of one or both of the nucleotides. In particular, G933S *improves* the affinity of both ATP and ADP compared to wild-type. It is important to note that G930S is dephosphorylated so that the minor effects on nucleotide specificity emanate from two modifications—GRL replacement and activation loop dephosphorylation. Figure 4 also displays the effects of serine replacement in the GRL glycines of PKA (open bars). Unlike v-Fps, all mutants in PKA lower ATP affinity compared to wild-type. Two of the mutants (G50S and G55S) also lower ADP affinity whereas replacement of the central glycine (G52S) has no effect on this product. This comparison indicates that the GRLs of v-Fps and PKA serve distinctive functions with regard to nucleotide recognition.

An important function of the GRL appears to be the governance of relative specificity between ATP and ADP. Figure 5 shows the relative specificity of wild-type and mutant forms of v-Fps for ATP compared to ADP (solid bars). In this plot, *y*-values greater than 1 imply that the enzyme prefers to bind ATP over ADP while values less than 1 imply a preference for ADP over ATP. While ADP binds with slightly better affinity to wild-type v-Fps than does ATP, G928S shows a strong preference for binding ATP over ADP while G933S shows a strong preference for binding ADP over ATP. Surprisingly, G930S demonstrates no preference for either nucleotide, but this mutant, unlike G928S and G933S, is dephosphorylated (Figure 1). While activation loop dephosphorylation is not expected to affect nucleotide affinity (*16*), synergistic effects between the GRL and activation loop could mask any specificity changes that may exist in the phosphorylated enzyme. Overall, the mutagenesis data suggest that the GRL is crucially important for controlling the nucleotide specificity of the enzyme. In fact, the opposing effects of G928S and G933S indicate that the loop balances the relative affinities of ATP and ADP so that neither is mainly preferred. This avoids deep energy wells or high transition state barriers in the reaction coordinate. As shown in Figure 5, the GRL of PKA appears to serve a different function (open bars). The glycines in PKA support ATP binding but play a reduced role in balancing the relative affinities of ATP and ADP. None of the GRL mutants for this enzyme improve the relative affinity of ATP compared to ADP.

CONCLUSIONS

The mutagenesis and kinetic data presented herein can be used to put forth an exciting role for the conserved glycines of the GRL in v-Fps. While all three glycines are important for maintaining efficient phosphoryl transfer to substrates, the second glycine (Gly-930) exerts the greatest influence on the k_3 step and the phosphorylation state of the activation loop. The molecular model for the v-Fps GRL suggests that these effects may be due to proximal influences on Asn-931 which is predicted to make two interactions with the β phosphate of ATP. None of the active mutants affect substrate binding in v-Fps unlike the analogous mutations in PKA where large effects are observed. In v-Fps, residue substitutions may either increase or decrease absolute ATP and ADP affinity but a comparison of the relative binding affinities of the wild-type and mutants for ATP and ADP suggests a unique role for this loop. The GRL finely balances the affinities of these two nucleotides with the apparent aim of inducing uniform binding. The energetic goal of this function may be to maintain reasonably high ATP affinity, to generate an environment that facilitates rapid phosphoryl transfer, and to expedite release of the product, ADP. In this capacity, the GRL may function as a "lid" to the nucleotide binding pocket. The flexibility of this "lid" is coupled with efficient catalysis so that disruptions in the natural dynamics of the loop lower the rate of chemistry in the active site and alter nucleotide association. While it is unclear how the glycines control specificity, the orientation of Asn-931 in the GRL could be a focal point.

REFERENCES

1. Hanks, S. K., and Hunter, T. (1995) *FASEB J. 9*, 576−596.
2. Zheng, J., Knighton, D. R., Ten Eyck, L. F., Karlsson, R., Xuong, N.-h., Taylor, S. S., and Sowadski, J. M. (1993) *Biochemistry 32*, 2154−2161.
3. Bossemeyer, D., Engh, R. A., Kinzel, V., Ponstingl, H., and Huber, R. (1993) *EMBO J. 12*, 849−859.
4. Hubbard, S. R. (1997) *EMBO J. 16*, 5572−5581.
5. Hemmer, W., McGlone, M., Tsigelny, I., and Taylor, S. S. (1997) *J. Biol. Chem. 272*, 16946−16954.
6. Grant, B. D., Hemmer, W., Tsigelny, I., Adams, J. A., and Taylor, S. S. (1998) *Biochemistry 37*, 7708−7715.
7. Zheng, J., Trafny, E. A., Knighton, D. R., Xuong, N.-h., Taylor, S. S., Ten Eyck, L. F., and Sowadski, J. M. (1993) *Acta Crystallogr., Sect. D 49*, 362−365.
8. Madhusudan, Trafny, E. A., Xuong, N.-h., Adams, J. A., Ten Eyck, L. F., Taylor, S. S., and Sowadski, J. M. (1994) *Protein Sci. 3*, 176−187.
9. Cheng, X., Shaltiel, S., and Taylor, S. S. (1998) *Biochemistry 37*, 14005−14013.

10. Hubbard, S. R., Wei, L., Ellis, L., and Hendrickson, W. A. (1994) *Nature 372*, 746−754.
11. Gish, G., McGlone, M. L., Pawson, T., and Adams, J. A. (1995) *Protein Eng. 8*, 609−614.
12. Wang, C., Lee, T. R., Lawrence, D. S., and Adams, J. A. (1996) *Biochemistry 35*, 1533−1539.
13. Saylor, P., Wang, C., Hirai, T. J., and Adams, J. A. (1998) *Biochemistry 37*, 12624−12630.
14. Adams, J. A. (1996) *Biochemistry 35*, 10949−10956.
15. Konkel, L., Hirai, T. J., and Adams, J. A. (2000) *Biochemistry 39*, 255−262.
16. Saylor, P., Hanna, E., and Adams, J. A. (1998) *Biochemistry 37*, 17875−17881.
17. MacDonald, I., Levy, J., and Pawson, T. (1985) *Mol. Cell. Biol. 5*, 2543−51.
18. Feldman, R. A., Gabrilove, J. L., Tam, J. P., Moore, A. S., and Hanafusa, H. (1985) *Proc. Natl. Acad. Sci. U.S.A.* 82, 2379−2383.
19. Yee, S.-P., Mock, D., Greer, P., Maltby, V., Rossant, J., Bernstein, A., and Pawson, T. (1989) *Mol. Cell. Biol. 9*, 5491−5499.
20. Yee, S.-P., Mock, D., Maltby, V., Silver, M., Rossant, J., Bernstein, A., and Pawson, T. (1989) *Proc. Natl. Acad. Sci. U.S.A. 86*, 5873−5877.
21. Maru, Y., Peters, K. L., Afar, D. E. H., Shibuya, M., Witte, O. N., and Smithgall, T. E. (1995) *Mol. Cell. Biol. 15*, 835−842.
22. Sadowski, I., Stone, J. C., and Pawson, T. (1986) *Mol. Cell. Biol. 6*, 4396−4408.
23. Jucker, M., McKenna, K., da Silva, A. J., Rudd, C. E., and Feldman, R. A. (1997) *J. Biol. Chem. 272*, 2104−2109.
24. Foster, D. A., Shibuya, M., and Hanafusa, H. (1985) *Cell 42*, 105−115.
25. Martell, A. E., and Smith, R. M. (1977) *Critical Stability Constants*, Vol. 3, Plenum, New York.
26. Shoemaker, D. P., and Garland, C. W. (1962) *Experiments in Physical Chemistry*, 2nd ed., McGraw-Hill, New York.
27. Weinmaster, G., Zoller, M. J., Smith, M., Hinze, E., and Pawson, T. (1984) *Cell 37*, 559−568.
28. Sadowski, I., and Pawson, T. (1987) *Oncogene 1*, 181−191.
29. Dixon, M. (1953) *Biochem. J. 55*, 170.
30. Grant, B., and Adams, J. A. (1996) *Biochemistry 35*, 2022−2029.
31. Adams, J. A., McGlone, M. L., Gibson, R., and Taylor, S. S. (1995) *Biochemistry 34*, 2447−2454.
32. Grant, B. D., Tsigelny, I., Adams, J. A., and Taylor, S. S. (1996) *Protein Sci. 5*, 1316−1324.
33. Skamnaki, V. T., Owen, D. J., Noble, M. E. M., Lowe, E. D., Lowe, G., Oikonomakos, N. G., and Johnson, L. N. (1999) *Biochemistry 38*, 14718−14730.
34. Cole, P. A., Burn, P., Takacs, B., and Walsh, C. T. (1994) *J. Biol. Chem. 269*, 30880−30887.
35. Cole, P. A., Grace, M. R., Phillips, R. S., Burn, P., and Walsh, C. T. (1995) *J. Biol. Chem. 270*, 22105−22108.
36. Sondhi, D., and Cole, P. A. (1999) *Biochemistry 38*, 11147−11155.
37. Shaffer, J., and Adams, J. A. (1999) *Biochemistry 38*, 12072−12079.

BI001216G